ACS OMEGA

Article

Cite This: ACS Omega 2018, 3, 18849−18856

http://pubs.acs.org/journal/acsodf

Low-Cost Strategy for the Development of a Rapid Electrochemical Assay for Bacteria Detection Based on AuAg Nanoshells

Lorenzo Russo,[†,‡] Juan Leva Bueno,[†] Jose Francisco Bergua,[†,‡] Monica Costantini,[§] Marco Giannetto,[§] Victor Puntes,[†,∥,⊥] Alfredo de la Escosura-Muñiz,[†] and Arben Merkoçi*[,†,‡,∥]

[†]Catalan Institute of Nanoscience and Nanotechnology (ICN2), CSIC and The Barcelona Institute of Science and Technology, Campus UAB, Bellaterra, 08193 Barcelona, Spain

[‡]Universitat Autònoma de Barcelona (UAB), Campus UAB, Bellaterra, 08193 Barcelona, Spain

[§]Department of Chemistry, Life Sciences and Environmental Sustainability, University of Parma, Parco Area delle Scienze 17/A, 43124 Parma, Italy

[∥]Vall d'Hebron Institut de Recerca (VHIR), 08035 Barcelona, Spain

[⊥]Institució Catalana de Recerca i Estudis Avançats (ICREA), P. Lluís Companys 23, 08010 Barcelona, Spain

Supporting Information

ABSTRACT: A low-cost strategy for the simple and rapid detection of bacterial cells in biological matrixes is presented herein. *Escherichia coli* and *Salmonella typhimurium* were chosen as model bacteria for the development of an electrochemical assay based on hollow AuAg nanoshells (NSs). By taking advantage of their electrocatalytic properties for the in situ generation of the electrochemical signal without the need of any other kind of reagent, substrate, or redox enzyme, high sensitivities (down to 10^2 CFU/mL) were achieved. Moreover, the recognition and discrimination of the model bacterial cells in the sample matrix was possible by relying solely on nonspecific affinity interactions between their cell walls and AuAg NSs surface, avoiding the use of expensive and fragile biological receptor. Compared to traditional, laboratory-based analytical tests available, this assay provides a promising proof-of-concept alternative that allows to obtain good sensitivities and selectivity in very short times in addition to the low cost.

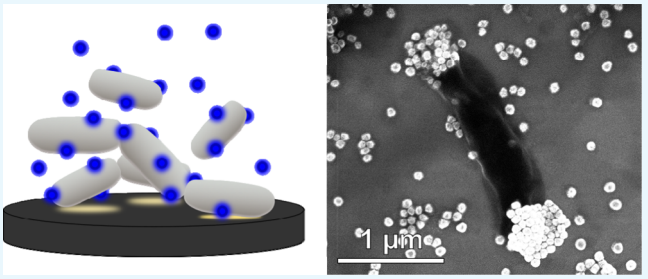

INTRODUCTION

Bacterial resistance to antimicrobials is considered widely the most urgent health issue the world is facing in the coming years.[1] Nowadays, the choice to prescribe antibiotics is rarely based on definitive diagnoses, which generally require laboratory-based analytical test (i.e., polymerase chain reaction (PCR), traditional plate counting), often consisting of days-long procedure characterized by high costs and the need for highly trained and skilled personnel. Effective, rapid, low-cost diagnostic tools are needed for guiding optimal use of antibiotics in human and animal medicine and, also in the form of point-of-care (POC) devices. Such tools should be easily integrated into clinical, pharmacy, and veterinary practices as high-throughput screening methods for the early discrimination between bacterial and viral infections.[2] In this context, nanotechnology has proven to be extremely successful in providing innovative and advantageous solutions to overcome the conventional in vitro diagnostic intrinsic limitations through the rational design of advanced nanomaterials with suitable properties and functionalities.[3−6] Among them, nanomaterials with unique electrochemical and electrocatalytic properties have been introduced as signal-amplification carriers or direct signal-generating elements to increase sensitivities and enhance analytic performances.[7−9]

The cost of diagnostics technologies is on the other hand one of the fundamental global health aspects to be considered for accessing the market with competitive and sustainable products.[10] Indeed, recognition elements found on the few POC electrochemical biosensors available consist fundamentally of biomolecules (i.e., enzymes, nucleic acids, antibodies), which represent one of the largest fraction of the total production cost.[11] Besides their unmatched specificity and selectivity, several drawbacks, such as high production cost and high susceptibility to environmental conditions (i.e., pH, temperature, metal cations, fouling agents, metabolites) can limit their applicability, especially when integrated into POC devices.[12] Exploiting instead the catalytic properties of electroactive nanomaterials presents a number of advantages, such as a lower production cost and engineering, ease of mass production, and a higher stability both in working conditions and long-term storage.[13−15]

Received: September 20, 2018
Accepted: December 3, 2018
Published: December 31, 2018

The aim of this work is therefore to employ the unique electrocatalytic properties of AuAg nanoshells (NSs)[16] for the quantitative detection of two model bacteria, *Escherichia coli* and *Salmonella typhimurium* (*Salmonella*). The ability to tune precisely their morphology and metal composition grants AuAg NSs with increased resistance to chemical oxidation while allowing them to generate a strong electrochemical signal. These unique features, together with high colloidal stability and large surface area, make AuAg NSs extremely promising materials to be employed as electrochemical labels in biosensors applications. Although AuAg NSs have been applied previously as nanostructured carriers for intracellular drug delivery and as surface enhanced Raman scattering labels for optical detection,[17,18] to the best of our knowledge, no similar reports of the use of this class of particles as electrochemical reporters have been published yet. Moreover, in our system, the detection of bacterial cells is achieved without the use of any biological receptor, basing it instead on nonspecific interactions between the AuAg NSs and the intrinsically highly differentiated bacterial cell surfaces. This approach, also experimented elsewhere,[19,20] provides a promising proof of concept for the development of a low-cost, robust electrochemical assay reaching high sensitivities (down to 10^2 CFU/mL) in very short times (within 10 min) compared to the available commercial *E. coli* POC assays and recently reported nanoparticles-based electrochemical detection techniques.[21]

RESULTS AND DISCUSSION

Electrochemical Properties of AuAg NSs. AuAg nanoshells consist of a hollow structure composed of a gold−silver alloy shell, which encloses an inner cavity. Their synthesis, based on a modified galvanic replacement reaction (GRR) reported previously by our group,[22] allows to precisely control both the morphology and the relative amount of the two noble metals. Figure 1A shows the transmission electron microscopy (TEM) micrographs of the product of the GRR displaying highly monodisperse hollow AuAg NSs of ca. 60 nm diameter, with a thin outer shell of ca. 10 nm thickness. The hollow particles bear a poly(vinyl pyrrolidone) (PVP) layer adsorbed on their surface during their synthesis, a hydrosoluble polymer, which provides enhanced colloidal stability without compromising their electrochemical properties.

Conventionally, noble-metal and semiconductor nanoparticles applied so far as electrochemical labels require strong oxidants or acids to generate their corresponding cationic species through corrosion, which can then be detected electrochemically through common voltammetric techniques.[23] Translating these technologies into electrochemical diagnostic platforms for commercial use becomes therefore extremely difficult due to the danger implied in handling these corrosive reagents. Although Ag NPs are instead prone to corrosion, they have found limited practical use due to severe susceptibility to oxidation,[24] resulting in limited durability and reproducibility in many biorelated applications. Thus, AuAg NSs were chosen as electrochemical signaling tool, thanks to their ability to generate an electrochemical signal in the presence of mild oxidizing agents, as demonstrated recently by our group.[16] The exposure of AuAg NSs to relatively high concentrations of nucleophilic halides and dissolved oxygen, typically found in most biological matrixes, is sufficient for activating their electrochemical properties: thanks to the residual Ag atoms contained in AuAg NSs cores, whose

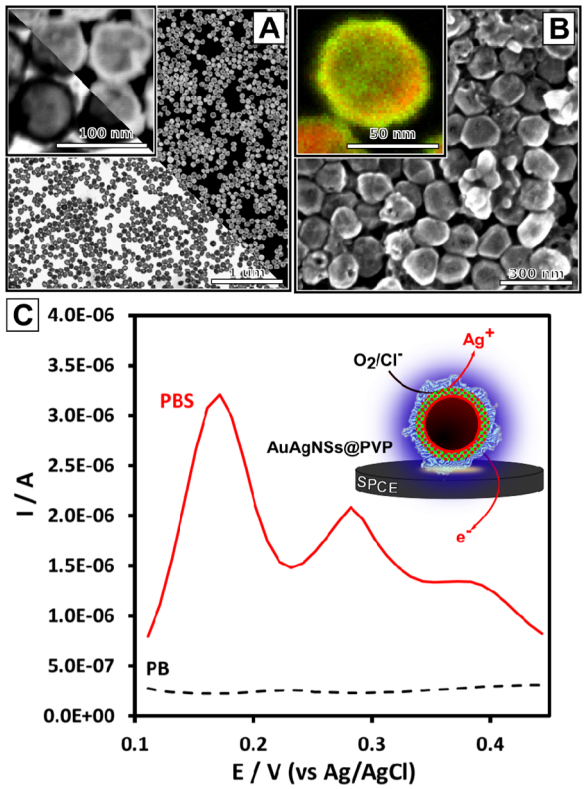

Figure 1. (A) TEM and high-angle annular dark-field scanning transmission electron microscopy (HAADF-STEM) micrographs of highly monodisperse 60.0 ± 4.4 nm AuAg NSs composed of a thin (≈10 nm) shell with a smooth surface and a large (≈40 nm) internal void. (B) Scanning electron microscopy (SEM) AuAg NSs surface characterization and HAADF-STEM elemental distribution micrographs of a single AuAg NS (inset; Au: green, Ag: red). At the final stage of GRR, Ag is found both in the Au-rich alloy outer thin shell and the inner particle surface in its metallic form. (C) Comparison of differential pulsed voltammetries (DPVs) of AuAg NSs in different buffers. The potential scan run in phosphate buffer saline (PBS) (red curve) causes the anodic stripping signal of Ag to appear at +0.16 V vs Ag/AgCl. When instead AuAg NSs are measured in phosphate buffer (PB) 10 mM pH 7.5 (black dashed curve), no relevant anodic current is observed. In the absence of chlorides in the matrix, no Ag corrosion is possible and therefore no stripping detection can be carried out.

amount can be precisely controlled during synthesis[22] (Figure 1B), Ag^+ cations are generated by corrosion without compromising the particles' structural stability, and anodic stripping analysis can be carried out for their detection.[16] Figure 1C shows the DPVs of AuAg NSs in PBS (red curve), showing a relatively strong and defined anodic peak at +0.16 V vs Ag/AgCl, completely absent instead when the same measurement is performed in PB (black dashed curve), that is, without chlorides in solution. A secondary oxidation peak is also observed at more positive potentials (+0.28 V vs Ag/AgCl), corresponding to the oxidation of alloyed Ag found in the outer shell of the particles.[16] These findings not only confirm the electrochemical mechanism of the current generation described above but also make AuAg NSs a promising substitute of natural redox enzymes as electrochemical labels for sensing applications.

We investigated systematically the different experimental parameters involved in the DPV measurement for optimizing the sensitivity of the system. First, Ag corrosion was monitored during this time to maximize the amount of Ag^+ cations

DOI: 10.1021/acsomega.8b02458
ACS Omega 2018, 3, 18849−18856

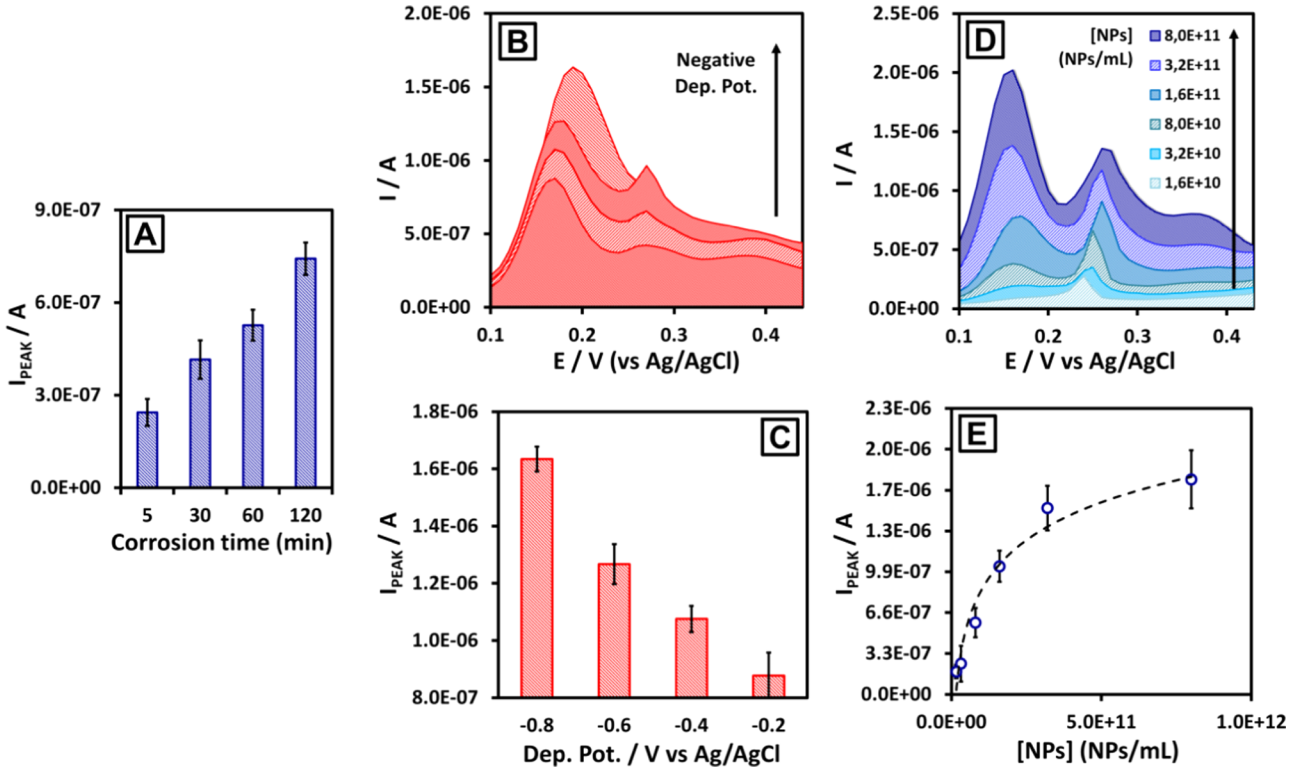

Figure 2. A) Time of residence of AuAg NSs in the oxidant matrix affects the anodic stripping current of Ag. Five minutes after mixing the hollow nanocrystal solution with PBS 10 mM pH 7.5, a relatively intense DPV current is obtained. Higher corrosion times allow to further enhance the current signal up to 4-fold for 120 min. (B, C) Effect of DPVs' initial deposition potential on the anodic stripping wave of Ag on screen printed carbon electrodes (SPCEs). (D, E) The dependency of the anodic stripping current on AuAg NSs' concentration is analyzed by running the DPVs of solution of increasing particles concentrations. The analytic peak (+0.16 V vs Ag/AgCl) intensity correlates positively with the increasing particles concentration (ranging from 1.6×10^{10} to 8.0×10^{11} NPs/mL), showing a logarithmic trend due to diffusion toward the electrode surface.

generated and, therefore, the corresponding anodic stripping current produced for a fixed amount of AuAg NSs (Figure 2A).

As expected, a higher residence time of the particles in the saline buffer before measurement causes a greater degree of Ag corrosion and therefore produces a stronger anodic current. Although the strongest signal was obtained for longer times (2 h), a 5 min long corrosion in the sample matrix was considered enough for generating the necessary signal intensity for the development of a rapid assay able to compete with traditional ones. This parameter could in theory be further optimized by increasing the total surface area available for chloride corrosion, for instance, by tuning the particles synthesis so to obtain a porous alloys shell.[22] It is worth mentioning that, despite the high salinity of the medium, no AuAg NSs aggregation is observed, thanks to the steric stabilization provided by the PVP coating (study of AuAg NSs colloidal stability can be found in Figure S1).

Second, the effect of the deposition potential, which is the negative potential applied at the beginning of the measurement needed for reducing Ag^+ onto the electrode surface,[25] was also analyzed. The DPVs of AuAg NSs solutions at a fixed concentration were therefore run by applying different deposition potentials before the measurement, namely, −0.2, −0.4, −0.6, and −0.8 V vs Ag/AgCl.

As shown in Figure 2B, varying the applied reduction potential does not seem to affect relevantly the oxidation peak's shape, apart from a slight shift in the peak position. On the contrary, a clear positive correlation between the applied deposition potential and the anodic current recorded at 0.16 V vs Ag/AgCl is observed (Figure 2C), resulting in increased current intensities up to 2-fold for −0.8 V vs Ag/AgCl. Remarkably, the possibility to reduce Ag^+ by applying more positive deposition potentials than silver's formal reduction one (Ag^+ reduction potentials = 0.7996 V)[26] depends on the ability of AuAg NSs to catalyze the underpotential deposition of Ag^+ on their surfaces, as recently discovered by our group.[16] This electrocatalytic effect is directly dependent on the particles' composition and morphology and can be tuned by modifying their synthesis.[22] Even though the highest signal obtained through this mechanism was found when using a deposition potential of −0.8 V vs Ag/AgCl, using less negative ones led to an improvement in the overall reproducibility of the measurement. In these conditions, in fact, Ag/AgCl pseudoreferences electrodes, known to display stability issues in electrolytes containing high chlorides concentrations,[27] showed a higher reproducibility. Figure S2 shows the behavior of the pseudoreference Ag/AgCl electrode vs the initial deposition potentials used. Besides the expected reference oxidation peak (≈0.0 V vs Ag/AgCl), the appearance of a satellite one when applying more negative deposition potentials (−0.4, −0.6, −0.8, and −1.0 V vs Ag/AgCl) was considered a probable cause of the reproducibility problems encountered. Using milder reduction potentials during the DPV measurement (−0.2 V vs Ag/AgCl) allows instead to completely avoid this effect. Moreover, the possibility to use AuAg NSs as electrochemical labels without the need to apply highly negative reduction potentials during the deposition step represents a further advantage because it eliminates the risk of

DOI: 10.1021/acsomega.8b02458
ACS Omega 2018, 3, 18849−18856

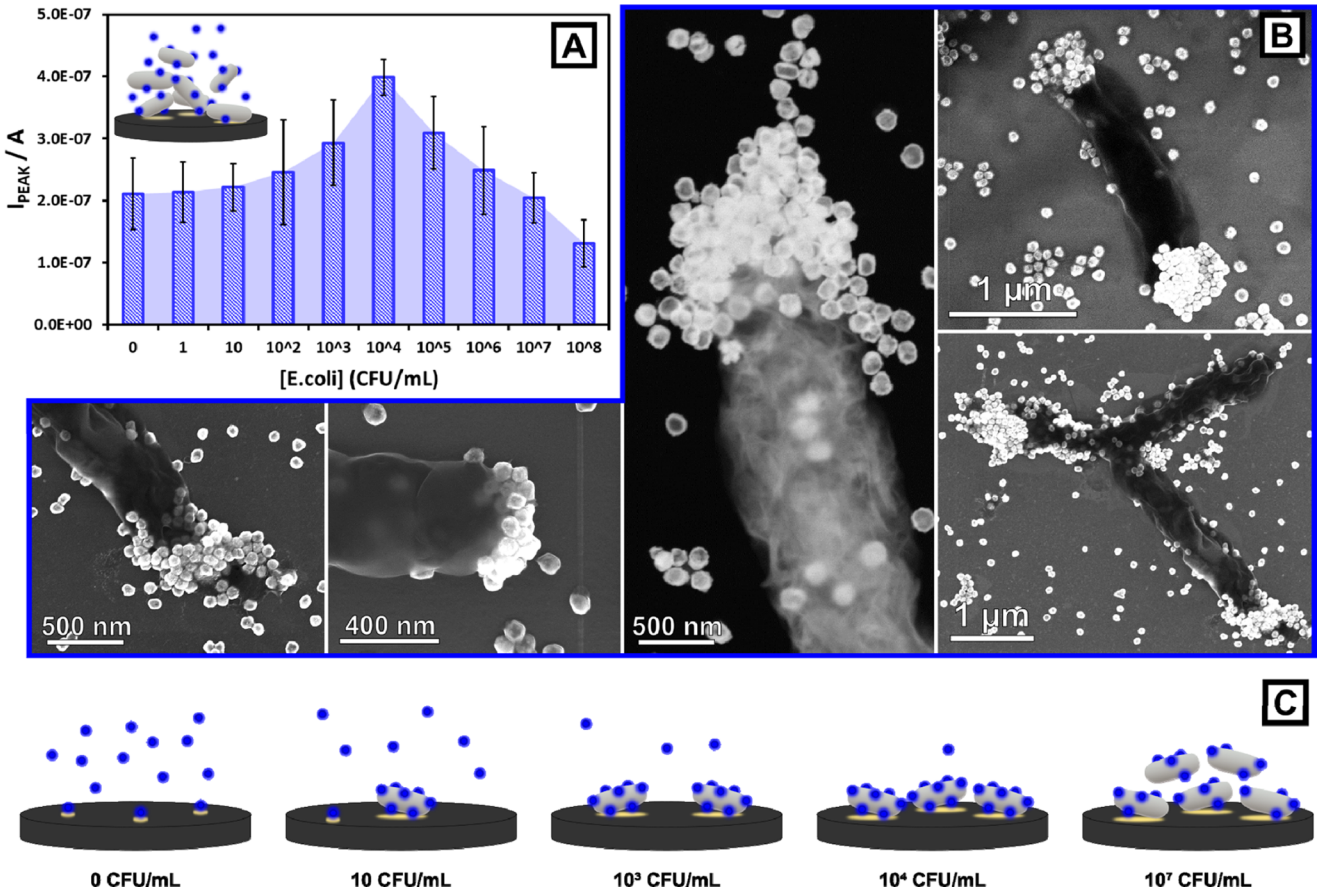

Figure 3. (A) *E. coli* detection through incubation with AuAg NSs and DPV measurement (bacteria cells concentration ranging from 10^1 to 10^8 CFU/mL). Error bars represent measurement standard deviation (n = 5), whose relatively high value are a result of the bacteria quantification (OD_{600}) high error. (B) STEM images (dark field and SEM) of *E. coli* cells decorated with AuAg NSs after incubation and differential centrifugation. (C) Affinity-based detection mechanism, depicting AuAg NSs (blue) and *E. coli* cells (gray) coming into contact with the electrode surface.

interference from redox-active species easily found in biological matrixes.

Finally, the correlation between AuAg NSs concentration and the measured electrochemical signal was studied by recording the anodic stripping peak intensity at +0.16 V while varying particles' concentration up to a 5-fold increase. As shown in Figure 2D,E, the electrochemical signal follows an increasing trend for the lower range of concentrations, after which it reaches a saturation plateau. This behavior is reasonably compatible with the electrochemical mechanism described above, considering that because no NSs immobilization over the electrode surface is carried out before the measurement, the diffusion rate of NSs toward the electrode surface will set an upper limit for the electron transfer and only the fraction of particles found in close proximity of the electrode surface will provide a detectable signal.[28] This setup allows detection of AuAg NSs down to a limit of detection of 5.6×10^{10} NPs/mL, but further improvement in sensitivity could be achieved by implementing longer deposition or corrosion steps.

Bacteria Detection. Conventional methods for specific quantification and differentiation of microbial cells use either selective culturing media, which can take up to several days to distinguish a positive from a negative sample, or molecular biology techniques, which instead target mainly intracellular biomarkers (i.e., proteins, nucleic acids) and therefore require complex and time-consuming procedures for extraction, amplification, and revelation (i.e., immunolabeling, PCR).[29] A less explored strategy for cell sensing focuses instead on the extracellular complex array of macro/biomolecules expressed on bacterial cell walls (i.e., phospholipids, lipopolysaccharides). Such sensing strategy takes advantage of the chemical fingerprint of these complex moieties to generate a nonspecific but selective response relying on the differential binding affinities between different nanoprobes and bacterial cells, thus without the need of costly biological receptors (i.e., antibodies, peptides, and nucleic acids).[20,30,31] This approach has been shown already to be a viable and promising one for their rapid detection and identification with minimal processing.[19,32]

The general protocol herein adopted for bacteria detection consists in mixing a solution of a model bacterial strain of *E. coli* at a given concentration (ranging from 10^1 to 10^8 CFU/mL) with PVP-coated AuAg NSs at a final concentration of 1.6×10^{11} NPs/mL, incubating the mixture for 5 min in PBS 10 mM pH 7.4 and then rapidly depositing it onto SPCEs to run a DPV, as described in the Experimental Section. The variation in anodic stripping current at +0.16 V, generated by the controlled corrosion of AuAg NPs in PBS, was then correlated with the concentration of *E. coli* cells (Figure 3A), revealing an initial increase in intensity up to a concentration of 10^4 CFU/mL, followed by a steep decrease in the peak current for higher ones. For *E. coli* concentrations higher than 10^6 CFU/mL, the

DOI: 10.1021/acsomega.8b02458
ACS Omega 2018, 3, 18849−18856

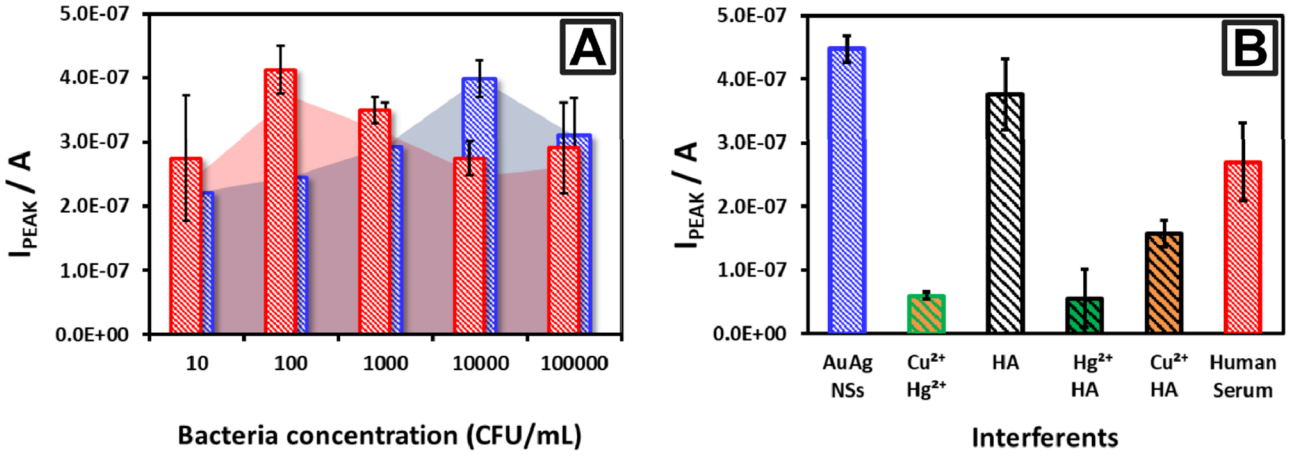

Figure 4. (A) Peak current profiles for different concentrations of *E. coli* (blue) and *Salmonella* (red): without the use of any specific receptor, affinity-based interactions between PVP-coated AuAg NSs and bacteria cell walls allow to selectively discriminate between the two species. (B) Peak currents recorded for assays run on samples containing *E. coli* suspension of 10^4 CFU/mL in the presence of different interfering species, namely, humic acid (HA), mercury (Hg^{2+}) and copper (Cu^{2+}) ions, and human serum.

voltammetric signal displays values lower than the blank ones. This peculiar current profile, encountered also in a previous work,[33] can be explained considering the bacteria's ability to "capture" the electroactive NPs in a solution through the nonspecific affinity interactions between PVP-coated AuAg NSs and the microorganisms' cell walls. As confirmed by the ζ-potential measured at three different pHs (Table S1), AuAg NSs colloidal stabilization is electrosteric, which is caused both by the electrostatic repulsion due to the negative surface charge (−24.5 ± 0.31 mV at pH = 7.5) and the steric interaction provided by the PVP adsorbed layer. Interestingly, this same layer appears to be also responsible for the nonspecific interaction between AuAg NSs in a solution and *E. coli* cell wall: as shown in the STEM micrographs of *E. coli* cells incubated with PVP-coated AuAg NSs (Figure 3B), the hollow nanocrystals seem to stick and accumulate on the bacterial cell wall extremities, probably thanks to the weak but additive interactions between the coating polymer and the extracellular macromolecules (i.e., phospholipids, lipopolysaccharides, and flagellar proteins). This kind of nonspecific interactions has been showed to be favored by the relatively hydrophobic character of both the extracellular macromolecules expressed and PVP, which is somehow able to screen the electrostatic repulsion between the negatively charged objects.[34−36] This attachment is not permanent, given the reversible nature of the weak interactions involved, but it is sufficient to label the bacterial cells with electrochemical reporters: after incubation of bacteria suspension with AuAg NSs, all the samples were purified through differential centrifugation[37] to separate the bacteria−particles complexes formed from the unattached ones (the presence in Figure 3B STEM images of free particles is likely caused by the later detachment during solvent evaporation upon sample preparation).

During the electrochemical assay, once the suspension of AuAg NSs-decorated bacteria in PBS is deposited on the electrode, cells quickly start to sediment, bringing the captured particles in contact with the electrode surface. For bacterial concentration ranging from 10^1 to 10^4 CFU/mL, the number of active electrochemical reporters found at the electrode surface is increased compared to the blank sample (Figure 3C, "0 CFU/mL") (in the absence of any cell, only the NPs in close proximity or contact with the electrode surface are able to provide an electrochemical signal). By increasing the concentration of cells, more particles can attach to the bacteria cell walls and thus reach the vicinity of the electrode surface, increasing the anodic stripping current of silver generated from the NSs (Figure 3C, "10^1−10^4 CFU/mL"). The electrochemical signal though reaches a maximum and then starts to decrease again for higher *E. coli* concentrations due to the depletion of free NPs in solution. In this second regime, the bacterial cells compete for capturing the limited amount of AuAg NSs, which are now distributed over a larger surface area, and hinder this way the electron transfers to the electrode surface (Figure 3C, "10^7 CFU/mL"). This particular electroanalytical response could be further improved for developing a more robust and reliable method for bacteria detection by performing a set of serial dilutions of the sample, where observing an increase rather than a decrease in current would correspond to a precise range of microbial concentrations, as demonstrated in Figure S3.

To test the selectivity of this detection strategy, a second model bacterial strain, *S. typhimurium*, was submitted to the same detection methodology. The current-vs-concentration profile obtained by incubating *Salmonella* cells with AuAg NSs (Figure 4, red bars) resulted in substantial similarity to the one observed with *E. coli* (Figure 4, blue bars), although reaching the maximum current intensity for lower bacteria concentrations. This differentiation between the two electrochemical responses can be explained by taking into account that the two bacterial species possess analogous but dissimilar variety and type of surface functional macromolecules expressed on their cell walls.[20] Their distinct functionalities will determine the degree of interaction with the functional macromolecules present on the particles surface, depending for instance on the intrinsic availability of hydrogen bonds donors or their hydrophobic character. As a consequence, the average ratio between the number of electrochemical reporters per bacterial cell will vary between different species. When incubating *Salmonella* cells with AuAg NSs, the overall sum of weak, nonspecific affinity interactions with the PVP-coated NPs corresponds to a distinct capture efficiency and NPs/bacteria ratio compared to the *E. coli* characteristic one, shifting, in other words, the bacteria concentration at which the capture effect reaches its maximum. This behavior, already reported

DOI: 10.1021/acsomega.8b02458
ACS Omega 2018, 3, 18849−18856

previously for PVP-coated AgNPs,[33,36,32] not only confirms the signal modulation mechanism proposed (Figure 3A,C) but also demonstrates the proof of concept for the feasibility of a semispecific assay able to discriminate between different pathogenic organisms without recurring to highly specific but also costly and fragile biological receptors. It is worth mentioning that this intrinsic affinity is obtained without the help (and notably the cost) of any kind of antibody or other bioreceptor, and that it could be in theory improved significantly by screening the nonspecific affinity of different coating polymers toward a particular bacterial cell species.[30,38]

For further testing the capability of this assay to distinguish and quantify different bacterial strains in complex mixtures containing both *E. coli* and *Salmonella*, a set of experiments were run (Figure S4). The results obtained show clearly that the assay in its current proof-of-concept format is not able to distinguish univocally between different compositions of the two model bacterial strains without constructing the whole concentrations profile. Nevertheless, it seems that the influence of *Salmonella* on the current generation mechanism, which is the capture of AuAg NSs in a solution through their nonspecific adsorption onto bacterial cells, is stronger than that of *E. coli*. This behavior gives additional clues about the different affinities of bacterial cell walls for AuAg NSs and could be used to further tune the hydrophobicity of the coating polymer toward a better selectivity of the assay.

To test the specificity in complex samples, we performed the assay over a suspension of 10^4 CFU/mL *E. coli* in the presence of two different kinds of interfering species. To check the specificity in the presence of large bio-macromolecules, the assay was run first in a duplicate experiment in human serum (Figure 4B, human serum), given the potential applicability of this assay in biological samples, and in the presence of humic acid (4 mg/L) (Figure 4B, HA), the major component of river waters' total organic carbon,[39] for application in environmental sensing. In the first case, the oxidation current peak at +0.16 V vs Ag/AgCl decreased in comparison to the control sample (Figure 4B, AuAg NSs), probably due to the formation of a protein corona around AuAg NSs,[40] which could either hinder the electron transfer to the electrode or directly lower the hollow nanocrystals' affinity for the macromolecules expressed onto the bacteria cell wall. Because the electrochemical quenching was not complete, this issue could be easily overcome by tuning the amount of AuAg NSs used in the assay to obtain a stronger current. In the case of humic acid instead, even though a slight decrease in the average intensity is observed, AuAg NSs seem to preserve their electrochemical properties, possibly due to the different chemical nature of humic substances, which makes them more stable in a solution and less prone to adsorption.[39] A second set of experiment was run to test the resilience of the assay to the presence of heavy metals, a common contaminant in river waters. Copper and mercury (2 and 0.006 mg/L, respectively)[41] salts were therefore chosen as interfering species because their oxidation potentials fall well within the potential window used in the assay. The electrochemical properties of AuAg NSs were this time completely quenched, both in the presence of metals and when either of them was used. Hg^{2+} was shown to quench the redox behavior completely, whereas Cu^{2+} resulted in a milder suppression. This effect can be easily explained taking into account the formation of amalgams between these cations and the noble metals, Au and Ag, constituting of the hollow nanostructures, as well as other deposition effects.[42,43]

CONCLUSIONS

In this work, we propose a low-cost strategy for the simple and rapid detection of bacterial cells in biological matrixes based on the use of hollow AuAg NSs as novel electrochemical reporters. Through a rapid electrochemical test (<10 min), the model bacterial strain *E. coli* was quantified down to a concentration of 10^2 CFU/mL using low-cost, one-use SCPEs as the sensing platform. The protocol developed does not need any additional reagent, substrate, or redox enzyme for generating the electrochemical signal, which is provided in situ by the controlled corrosion of AuAg NSs caused by the matrix salinity. Moreover, discrimination between *E. coli* and *S. typhimurium* was achieved without the use of any biological receptor but through nonspecific affinity interactions between the microorganism cell wall and AuAg NSs' surface, providing selectivity at a minimal operative and reagents cost. This work provides a promising proof of concept for the development of low-cost, rapid electrochemical assay for bacteria quantification able to compete with conventional costly and time-consuming laboratory analyses.

EXPERIMENTAL SECTION

Silver nitrate ($AgNO_3$), trisodium citrate ($Na_3C_6H_5O_7$), tannic acid ($C_{76}H_{52}O_{46}$), $HAuCl_4{\cdot}3H_2O$ (99%), poly(vinyl pyrrolidone) $(C_6H_9NO)_n$ $M_w \approx 55\,000$ (PVP), human serum, and humic acid were purchased from Sigma-Aldrich. Copper nitrate trihydrate and mercury nitrate standard solutions were purchased from Panreac. All the chemicals were used as received without further purification. Distilled water passed through a Millipore system (ρ = 18.2 MΩ) was used in all the experiments. All the glassware were first rinsed with acetone and then with Millipore water before use. Buffers solutions were prepared in Milli-Q water obtained from a Millipore system Vent Filter MPK01. Both buffers, phosphate buffer (PB) and phosphate buffer saline (PBS), were prepared at a concentration of 0.01 M and at pH 7.4. PB was prepared by mixing sodium-phosphate monobasic hydrogen along with sodium-phosphate dibasic hydrogen in the desired proportion; PBS was purchased from Sigma-Aldrich in tablets.

Screen printed carbon electrodes (SPCEs) were fabricated with a semiautomatic screen-printing machine DEK248 (DEK International, Switzerland). Electrodes were printed over Autostat HT5 polyester sheets (McDermid Autotype, U.K.) using Carbon Sensor Paste C2030519P4 for working and counter electrodes, Gray Dielectric Paste D2070423P5 silver/silver chloride ink for reference electrode, and Minico 7000 Blue insulating ink (Acheson Industries, The Netherlands) to insulate the contacts and define the sample interaction area.

All the nanoparticles were characterized by UV−vis spectroscopy (Perkin-Elmer "Lambda25"), dynamic light scattering (Malvern Zetasizer), transmission electron microscopy (TEM), and scanning electron microscopy (SEM) (FEI Magellan 400L). The high-resolution TEM images were obtained using a FEI Tecnai F20 field-emission gun microscope with a 0.19 nm point-to-point resolution operated at 200 keV.

The electrochemical experiments were performed by AUTOLAB PGSTAT302N (Echo Chemie, The Netherlands) potentiostat/galvanostat, which was connected to a computer and monitored by GPES software. All the experiments were performed at room temperature. The SCPEs were connected with the potentiostat through a homemade connector. The

DOI: 10.1021/acsomega.8b02458
ACS Omega 2018, 3, 18849−18856

general protocol for the electrochemical measurements of nanoparticles (NPs)-containing samples is as follows: 10 μL of AuAg NSs suspension at a nominal concentration of 1.6×10^{11} NPs/mL, unless specified otherwise, were transferred into a plastic 1.5 mL Eppendorf tube containing 50 μL of a bacteria suspension in PBS 10 mM pH 7.4 with a given bacteria colony forming units (CFU)/mL. After incubation in the saline matrix for a given time and under stirring at 600 rpm in a thermoshaker at 25 °C, 50 μL of the mixture was displaced onto the SPCE so as to cover the three electrodes. Differential pulsed voltammetry (DPV) was run: after applying a fixed deposition negative potential for 60 s, voltage was scanned between −0.05 and +0.4 V with 0.01 V step potential. Cyclic voltammetries were recorded in the same conditions scanning from −0.8 to +0.3 V at 100 mV/s scan rate with 0.005 V step potential.

E. coli O157:H7 (CECT 4783) and *Salmonella enterica* subsp. *enterica* serovar Typhimurium LT2 (CECT 722 T) strains were obtained from "Colección Española de Cultivos Tipo" (CECT). *E. coli* stock cultures were kept in trypticase soy agar (TSA) sloped tubes at 4 °C and stored in these conditions no longer than 2 months. To start up the culture, some *E. coli* colonies were transferred from TSA to trypticase soy broth tubes at 37 °C for 24 h for bacterial growth. Next day, a small fraction of the new grown bacterial culture was taken with a loop (≈1 μL) and carried to a TSA plate. Again, bacteria were allowed to grow at 37 °C for 24 h. Finally, a glass tube was filled up with 0.01 M PBS and some colonies were introduced into the tube. Bacteria solution was vortexed and OD was measured using McFarland standards: a value of 0.5 indicated a bacterial density of around 1.5×10^8 CFU/mL. *E. coli* living cells were eventually subjected to a sharp temperature increase (80 °C) for 20 min to kill without compromising the outer cell wall structure. The same process was carried out for *Salmonella* strain.

■ ASSOCIATED CONTENT

Supporting Information

The Supporting Information is available free of charge on the ACS Publications website at DOI: 10.1021/acsomega.8b02458.

Stability study for AuAg NSs; stability study for Ag/AgCl pseudoreference electrode; Z-potential of AuAg NSs; dilution method for electrochemical assay; multicomponent samples analysis (PDF)

■ AUTHOR INFORMATION

Corresponding Author

*E-mail: arben.merkoci@icn2.cat.

ORCID

Arben Merkoçi: 0000-0003-2486-8085

Notes

The authors declare no competing financial interest.

■ ACKNOWLEDGMENTS

This work was carried out within the "Doctorat en Quìmica" PhD programme of Universitat Autònoma de Barcelona, supported by the Spanish MINECO (MAT2015-70725-R) and from the Catalan Agència de Gestió d'Ajuts Universitaris i de Recerca (AGAUR) (2017-SGR-143). Financial support from the HISENTS (685817) Project financed by the European Community under H20202 Capacities Programme is gratefully acknowledged. It was also funded by the CERCA Program/Generalitat de Catalunya. ICN2 acknowledges the support of the Spanish MINECO through the Severo Ochoa Centers of Excellence Program under Grant SEV2201320295.

■ REFERENCES

(1) World Health Organization. *Global Action Plan on Antimicrobial Resistance*; WHO Press, 2015; pp 1−28.

(2) Drain, P. K.; Hyle, E. P.; Noubary, F.; Freedberg, K. A.; Wilson, D.; Bishai, W. R.; Rodriguez, W.; Bassett, I. V. Diagnostic Point-of-Care Tests in Resource-Limited Settings. *Lancet Infect. Dis.* **2014**, *14*, 239−249.

(3) Huang, X.; Liu, Y.; Yung, B.; Xiong, Y.; Chen, X. Nanotechnology-Enhanced No-Wash Biosensors for In Vitro Diagnostics of Cancer. *ACS Nano* **2017**, *11*, 5238−5292.

(4) Lee, W. G.; Kim, Y.-G.; Chung, B. G.; Demirci, U.; Khademhosseini, A. Nano/Microfluidics for Diagnosis of Infectious Diseases in Developing Countries. *Adv. Drug Delivery Rev.* **2010**, *62*, 449−457.

(5) Polavarapu, L.; Liz-Marzán, L. M. Towards Low-Cost Flexible Substrates for Nanoplasmonic Sensing. *Phys. Chem. Chem. Phys.* **2013**, *15*, 5288−5300.

(6) Bülbül, G.; Hayat, A.; Andreescu, S. Portable Nanoparticle-Based Sensors for Food Safety Assessment. *Sensors* **2015**, *15*, 30736−30758.

(7) Qiu, H.-J.; Li, X.; Xu, H.-T.; Zhang, H.-J.; Wang, Y. Nanoporous Metal as a Platform for Electrochemical and Optical Sensing. *J. Mater. Chem. C* **2014**, *2*, 9788−9799.

(8) Ambrosi, A.; Merkoçi, A.; de la Escosura-Muñiz, A. Electrochemical Analysis with Nanoparticle-Based Biosystems. *TrAC, Trends Anal. Chem.* **2008**, *27*, 568−584.

(9) Kelley, S. O.; Mirkin, C. A.; Walt, D. R.; Ismagilov, R. F.; Toner, M.; Sargent, E. H. Advancing the Speed, Sensitivity and Accuracy of Biomolecular Detection Using Multi-Length-Scale Engineering. *Nat. Nanotechnol.* **2014**, *9*, 969−980.

(10) Huckle, D. Point-of-Care Diagnostics: Will the Hurdles Be Overcome This Time? *Expert Rev. Med. Devices* **2006**, *3*, 421−426.

(11) El Harrad, L.; Bourais, I.; Mohammadi, H.; Amine, A. Recent Advances in Electrochemical Biosensors Based on Enzyme Inhibition for Clinical and Pharmaceutical Applications. *Sensors* **2018**, *18*, 164.

(12) Rocchitta, G.; Spanu, A.; Babudieri, S.; Latte, G.; Madeddu, G.; Galleri, G.; Nuvoli, S.; Bagella, P.; Demartis, M. I.; Fiore, V.; et al. Enzyme Biosensors for Biomedical Applications: Strategies for Safeguarding Analytical Performances in Biological Fluids. *Sensors* **2016**, *16*, 780.

(13) Kotov, N. A. Inorganic Nanoparticles as Protein Mimics. *Science* **2010**, *330*, 188−189.

(14) Cheng, H.; Lin, S.; Muhammad, F.; Lin, Y. W.; Wei, H. Rationally Modulate the Oxidase-like Activity of Nanoceria for Self-Regulated Bioassays. *ACS Sens.* **2016**, *1*, 1336−1343.

(15) Wang, C.; Chen, W.; Chang, H. Enzyme Mimics of Au/Ag Nanoparticles for Fluorescent Detection of Acetylcholine. *Anal. Chem.* **2012**, *84*, 9706−9712.

(16) Russo, L.; Puntes, V.; Merkoçi, A. Tunable Electrochemistry of Gold-Silver Alloy Nanoshells. *Nano Res.* **2018**, 6336.

(17) Wang, Y.; Salehi, M.; Schütz, M.; Schlücker, S. Femtogram Detection of Cytokines in a Direct Dot-Blot Assay Using SERS Microspectroscopy and Hydrophilically Stabilized Au-Ag Nanoshells. *Chem. Commun.* **2014**, *50*, 2711−2714.

(18) Jang, H.; Kim, D. E.; Min, D. H. Self-Assembled Monolayer Mediated Surface Environment Modification of Poly-(Vinylpyrrolidone)-Coated Hollow Au-Ag Nanoshells for Enhanced Loading of Hydrophobic Drug and Efficient Multimodal Therapy. *ACS Appl. Mater. Interfaces* **2015**, *7*, 12789−12796.

(19) Miranda, O. R.; Li, X.; Garcia-Gonzalez, L.; Zhu, Z. J.; Yan, B.; Bunz, U. H. F.; Rotello, V. M. Colorimetric Bacteria Sensing Using a Supramolecular Enzyme-Nanoparticle Biosensor. *J. Am. Chem. Soc.* **2011**, *133*, 9650−9653.

DOI: 10.1021/acsomega.8b02458
ACS Omega 2018, 3, 18849−18856

(20) Chen, J.; Andler, S. M.; Goddard, J. M.; Nugen, S. R.; Rotello, V. M. Integrating Recognition Elements with Nanomaterials for Bacteria Sensing. *Chem. Soc. Rev.* **2017**, *46*, 1272−1283.
(21) Chen, J.; Jiang, Z.; Ackerman, J. D.; Yazdani, M.; Hou, S.; Nugen, S. R.; Rotello, V. M. Electrochemical Nanoparticle−enzyme Sensors for Screening Bacterial Contamination in Drinking Water. *Analyst* **2015**, *140*, 4991−4996.
(22) Russo, L.; Merkoçi, F.; Patarroyo, J.; Piella, J.; Merkoçi, A.; Bastús, N. G.; Puntes, V. Time- and Size-Resolved Plasmonic Evolution with Nm Resolution of Galvanic Replacement Reaction in AuAg Nanoshells Synthesis. *Chem. Mater.* **2018**, *30*, 5098−5107.
(23) Wan, Y.; Zhou, Y.-G.; Poudineh, M.; Safaei, T. S.; Mohamadi, R. M.; Sargent, E. H.; Kelley, S. O. Highly Specific Electrochemical Analysis of Cancer Cells Using Multi-Nanoparticle Labeling. *Angew. Chem., Int. Ed.* **2014**, *53*, 13145−13149.
(24) Zheng, Y.; Zeng, J.; Ruditskiy, A.; Liu, M.; Xia, Y. Oxidative Etching and Its Role in Manipulating the Nucleation and Growth of Noble-Metal Nanocrystals. *Chem. Mater.* **2014**, *26*, 22−33.
(25) Cloake, S. J.; Toh, H. S.; Lee, P. T.; Salter, C.; Johnston, C.; Compton, R. G. Anodic Stripping Voltammetry of Silver Nanoparticles: Aggregation Leads to Incomplete Stripping. *ChemistryOpen* **2015**, *4*, 22−26.
(26) Douglas, F.; Yañez, R.; Ros, J.; Marín, S.; De La Escosura-Muñiz, A.; Alegret, S.; Merkoçi, A. Silver, Gold and the Corresponding Core Shell Nanoparticles: Synthesis and Characterization. *J. Nanopart. Res.* **2008**, *10*, 97−106.
(27) Toh, H. S.; Batchelor-McAuley, C.; Tschulik, K.; Compton, R. G. Electrochemical Detection of Chloride Levels in Sweat Using Silver Nanoparticles: A Basis for the Preliminary Screening for Cystic Fibrosis. *Analyst* **2013**, *138*, 4292−4297.
(28) Kleijn, S. E. F.; Lai, S. C. S.; Koper, M. T. M.; Unwin, P. R. Electrochemistry of Nanoparticles. *Angew. Chem., Int. Ed.* **2014**, *53*, 3558−3586.
(29) Tamerat, N.; Muktar, Y. Application of Molecular Diagnostic Techniques for the Detection of *E. coli* O157:H7: A Review. *J. Vet. Sci. Technol.* **2016**, *7*, 362.
(30) Jiang, Z.; Le, N. D. B.; Gupta, A.; Rotello, V. M. Cell Surface-Based Sensing with Metallic Nanoparticles. *Chem. Soc. Rev.* **2015**, *44*, 4264−4274.
(31) Feng, Z. V.; Gunsolus, I. L.; Qiu, T. A.; Hurley, K. R.; Nyberg, L. H.; Frew, H.; Johnson, K. P.; Vartanian, A. M.; Jacob, L. M.; Lohse, S. E.; et al. Impacts of Gold Nanoparticle Charge and Ligand Type on Surface Binding and Toxicity to Gram-Negative and Gram-Positive Bacteria. *Chem. Sci.* **2015**, *6*, 5186−5196.
(32) Sepunaru, L.; Tschulik, K.; Batchelor-McAuley, C.; Gavish, R.; Compton, R. G. Electrochemical Detection of Single *E. coli* Bacteria Labeled with Silver Nanoparticles. *Biomater. Sci.* **2015**, *3*, 816−820.
(33) Hassan, A. R. H. A. A.; de la Escosura-Muñiz, A.; Merkoçi, A. Highly Sensitive and Rapid Determination of *Escherichia coli* O157:H7 in Minced Beef and Water Using Electrocatalytic Gold Nanoparticle Tags. *Biosens. Bioelectron.* **2015**, *67*, 511−515.
(34) El Badawy, A. M.; Silva, R. G.; Morris, B.; Scheckel, K. G.; Suidan, M. T.; Tolaymat, T. M. Surface Charge-Dependent Toxicity of Silver Nanoparticles. *Environ. Sci. Technol.* **2011**, *45*, 283−287.
(35) Song, J. E.; Phenrat, T.; Marinakos, S.; Xiao, Y.; Liu, J.; Wiesner, M. R.; Tilton, R. D.; Lowry, G. V. Hydrophobic Interactions Increase Attachment of Gum Arabic- and PVP-Coated Ag Nanoparticles to Hydrophobic Surfaces. *Environ. Sci. Technol.* **2011**, *45*, 5988−5995.
(36) Bondarenko, O.; Ivask, A.; Käkinen, A.; Kurvet, I.; Kahru, A. Particle-Cell Contact Enhances Antibacterial Activity of Silver Nanoparticles. *PLoS One* **2013**, *8*, No. e64060.
(37) Sousa, C.; Sequeira, D.; Kolen'Ko, Y. V.; Pinto, I. M.; Petrovykh, D. Y. Analytical Protocols for Separation and Electron Microscopy of Nanoparticles Interacting with Bacterial Cells. *Anal. Chem.* **2015**, *87*, 4641−4648.
(38) MacKenzie, D. A.; Sherratt, A. R.; Chigrinova, M.; Kell, A. J.; Pezacki, J. P. Bioorthogonal Labelling of Living Bacteria Using Unnatural Amino Acids Containing Nitrones and a Nitrone Derivative of Vancomycin. *Chem. Commun.* **2015**, *51*, 12501−12504.
(39) Frimmel, F. Aquatic Humic Substances. In *Biopolymers, Volume 1: Lignin, Humic Substances and Coal*; Wiley-VCH, 2001; pp 301−310.
(40) Barbero, F.; Russo, L.; Vitali, M.; Piella, J.; Salvo, I.; Borrajo, M. L.; Busquets-Fité, M.; Grandori, R.; Bastús, N. G.; Casals, E.; et al. Formation of the Protein Corona: The Interface between Nanoparticles and the Immune System. *Semin. Immunol.* **2017**, *34*, 52−60.
(41) Gorchev, H. G.; Ozolins, G. WHO Guidelines for Drinking-Water Quality. *WHO Chron.* **1984**, *38*, 104−108.
(42) Li, L.; Feng, D.; Fang, X.; Han, X.; Zhang, Y. Visual Sensing of Hg2+ Using Unmodified Au@Ag Core−shell Nanoparticles. *J. Nanostructure Chem.* **2014**, *4*, 117.
(43) Price, S. W. T.; Speed, J. D.; Kannan, P.; Russell, A. E. *Exploring the First Steps in Core − Shell Electrocatalyst Preparation: In Situ Characterization of Cu and Pd Shells on Supported Au Nanoparticles* **2011**, *133*, 19448−19458.

DOI: 10.1021/acsomega.8b02458
ACS Omega 2018, 3, 18849−18856